

# Measurement of the orientation of buffer-gas-cooled, electrostatically-guided ammonia molecules

Edward W. Steer<sup>a</sup>, Lorenzo S. Petralia<sup>a</sup>, Colin M. Western<sup>b</sup>, Brianna R. Heazlewood<sup>a,\*</sup>, Timothy P. Softley<sup>c</sup>

<sup>a</sup> Department of Chemistry, University of Oxford, Chemistry Research Laboratory, 12 Mansfield Road, Oxford OX1 3TA, United Kingdom

<sup>b</sup> School of Chemistry, University of Bristol, Cantock's Close, Bristol BS8 1TS, United Kingdom

<sup>c</sup> University of Birmingham, Edgbaston, Birmingham B15 2TT, United Kingdom

## ARTICLE INFO

### Article history:

Received 15 July 2016

In revised form 2 November 2016

Accepted 10 November 2016

Available online 11 November 2016

### Keywords:

Cold molecules

Quadrupole guide

Alignment

Ammonia

Polarisation

## ABSTRACT

The extent to which the spatial orientation of internally and translationally cold ammonia molecules can be controlled as molecules pass out of a quadrupole guide and through different electric field regions is examined. Ammonia molecules are collisionally cooled in a buffer gas cell, and are subsequently guided by a three-bend electrostatic quadrupole into a detection chamber. The orientation of ammonia molecules is probed using  $(2 + 1)$  resonance-enhanced multiphoton ionisation (REMPI), with the laser polarisation axis aligned both parallel and perpendicular to the time-of-flight axis. Even with the presence of a near-zero field region, the ammonia REMPI spectra indicate some retention of orientation. Monte Carlo simulations propagating the time-dependent Schrödinger equation in a full basis set including the hyperfine interaction enable the orientation of ammonia molecules to be calculated – with respect to both the local field direction and a space-fixed axis – as the molecules pass through different electric field regions. The simulations indicate that the orientation of  $\sim 95\%$  of ammonia molecules in  $J_K = 1_1$  could be achieved with the application of a small bias voltage (17 V) to the mesh separating the quadrupole and detection regions. Following the recent combination of the buffer gas cell and quadrupole guide apparatus with a linear Paul ion trap, this result could enable one to examine the influence of molecular orientation on ion-molecule reaction dynamics and kinetics.

© 2017 The Authors. Published by Elsevier Inc. This is an open access article under the CC BY license (<http://creativecommons.org/licenses/by/4.0/>).

## 1. Introduction

A prevailing goal in the study of reaction dynamics is to develop a complete understanding of the reaction process. Studying chemical reactions under cold conditions can provide control over the internal quantum state population distribution, which typically collapses down into the lowest few levels in small molecules at temperatures  $\leq 1$  K. The long-range intermolecular forces experienced by slow-moving molecules can also affect the orientation of reactants during the collision process – and thus influence the properties of the resulting products [1,2]. Over the past half century, the development of methodologies to control the spatial orientation of reactants has seen the investigation of steric effects [3] as well as the direct measurement of “molecular-frame” photofragment distributions [4,5].

Spatially orienting molecules can allow one to control the outcome of reactive collisions. This was demonstrated in 1976, with the introduction of molecular beam scattering experiments:  $\text{CH}_3\text{I}$

molecules were state-selected using a hexapole and aligned with a static field, before reacting with K atoms. The production of KI showed a strong dependence on whether the methyl group was oriented towards or away from the K atom [6]. Orientation effects have been demonstrated under ultracold conditions with KRb molecules held in an optical lattice trap. The  $2\text{KRb} \rightarrow \text{K}_2 + \text{Rb}_2$  reaction was suppressed when the dipoles of the KRb molecules were aligned, such that only unfavourable “side-by-side” collisions could occur; the reactive “head-to-tail” collisions were prevented and the reaction rate constant was significantly reduced from that recorded with no orientation of the reactants [7]. Recently, the total electronic angular momentum of  $\text{O}(^3\text{P}_2)$ ,  $\text{Ne}(^3\text{P}_2)$  and  $\text{He}(^3\text{S}_1)$  beams emerging from a bent magnetic guide have been found to exhibit a substantial degree of orientation to the quantisation axis – in spite of the absence of additional uniform magnetic fields after the guide [8]. A combination of weak fringe fields emanating from the guide, stray magnetic fields, and the way that the species are transmitted through the bent guide has been proposed as the cause of the observed orientation.

Electric fields serve to shift and split the energy levels of polar molecules, in addition to orienting the dipole moment of the

\* Corresponding author.

E-mail address: [brianna.heazlewood@chem.ox.ac.uk](mailto:brianna.heazlewood@chem.ox.ac.uk) (B.R. Heazlewood).

species. The orientation of dipoles can be considered from a classical or a quantum mechanical perspective. Classically, molecules tend to adopt the most stable (*i.e.* lowest energy) configuration, which sees the dipole moment orient parallel to the local electric field, although the rotational kinetic energy may be sufficient to overcome the orientational force. Quantum mechanically, the orientation of the dipole is governed by the change in the rotational wave function induced by the field [9]. The electric fields in a quadrupole (or hexapole) guide enable one to state-select molecules and to orient them in the local electric field, which is not uniform in direction within the quadrupole. Typically, molecules exiting the guide enter a homogeneous field region provided by parallel electrodes. This post-quadrupole applied field adiabatically reorients the molecules from the inhomogeneous field in the quadrupole to a fixed laboratory axis, as molecules follow the direction of the local field [6]. Thus symmetric top molecules can be state-selected and oriented in the laboratory frame through the combination of a quadrupole guide and static electric fields. However, if the transmission into the homogeneous field region involves passage through a near-zero-field zone, non-adiabatic transitions could lead to loss of orientation.

In this paper, we probe the orientation of cold ammonia molecules after they exit a quadrupole guide and enter a reaction chamber, designed ultimately for the study of cold ion-molecule collisions. (2 + 1) resonance-enhanced multiphoton ionisation (REMPI) spectroscopy is employed, with the laser polarisation axis aligned both parallel and perpendicular to the time-of-flight (ToF) axis to determine the molecular orientation. The extent to which ammonia molecules can be oriented in the experimental apparatus in this work, and the conditions necessary to achieve orientation, is examined using Monte Carlo simulations. The ultimate goal is to gain control over all ion-molecule reaction parameters. While there is significant scrambling of the orientation of ammonia molecules as they pass through the different electric field regions, amendments to the experimental apparatus provide conditions appropriate for preserving the orientation of polar symmetric top molecules. This presents the exciting prospect of controlling the translational energy, rotational population distribution and orientation of polar reactants as they undergo reactive collisions with cold ions confined in a linear Paul trap.

## 2. Experimental methods

### 2.1. Experimental apparatus

The experimental apparatus, based on the design of Sommer et al. [10], has been described in Ref. [11], hence only a brief description is provided here. Ammonia molecules, either  $\text{NH}_3$  or  $\text{ND}_3$ , are injected into a quadrupole guide after being collisionally cooled by helium buffer gas. A  $20 \times 40 \times 40$  mm (length  $\times$  height  $\times$  width) buffer-gas cell is attached to the second stage of a two-stage pulse-tube cryocooler. The buffer gas line thermalises with each of the nested temperature stages, and helium enters the cell at 6 K. The molecular line is thermally insulated from the cryogenic environment, with a small heating block ensuring that ammonia molecules enter the cell at 210 K. Ammonia molecules are cooled by collisions with helium buffer gas atoms in the cell, and pass out of the cell through an exit aperture. A 2 m-long three-bend electrostatic quadrupole then guides internally and translationally cold ammonia molecules (in low-field seeking states) through two differentially pumped regions and into a reaction chamber (see Fig. 1 of Ref. [11]). Previous work [11] has shown that a low rotational temperature, *ca.* 10 K, is maintained at the exit of the quadrupole guide. The transmission of the different

$J_K$  states through the quadrupole guide is discussed in detail in Ref. [11].

The quadrupole is assembled from hand-polished stainless steel rods with a circular cross section and 2 mm diameter. Voltages of  $\pm 5$  kV are applied to the quadrupole electrodes, achieving maximal field strengths of up to  $90 \text{ kV cm}^{-1}$  at the electrode surfaces. After exiting the guide, molecules pass through a grounded Ni mesh covering an area with a 20 mm diameter. The ammonia molecules subsequently pass through a repeller electrode (inner diameter 25 mm) and are intersected by a REMPI laser between the repeller and extractor plates (see Fig. 1). The resulting ions are accelerated into a flight tube and onto microchannel plates (MCPs) for detection.

### 2.2. Orientation of molecules

Electric (magnetic) fields are commonly used to orient molecules that have a permanent electric dipole moment (magnetic moment). For a symmetric top molecule, the interaction energy between a permanent dipole,  $\mu$ , and an external electric field,  $E$ , can be expressed in scalar terms as  $-\mu E \langle \cos \theta \rangle$ , where  $\langle \cos \theta \rangle = KM/J(J+1)$  and  $\theta$  is the angle between the dipole and the field axis [12].  $J$  is the total angular momentum quantum number excluding nuclear spin,  $K$  is the projection of  $\mathbf{J}$  onto the molecular axis, and  $M$  is the projection of  $\mathbf{J}$  onto the external field axis. Hence orientation effects are molecule and state dependent. The magnitude of the electric field in the quadrupole guide, which near the axis varies linearly with distance from the axis and is approximately independent of azimuthal angle, is more than sufficient to influence the orientation of ammonia molecules (except very close to the axis).

Between the quadrupole guide and the point of ionisation – specifically, at the entrance to the mesh – the quantisation axis is rapidly rotated from the inhomogeneous electric field in the quadrupole (perpendicular to the quadrupole axis) to the homogeneous field between the repeller and extractor plates (parallel to the quadrupole axis). The extent to which ammonia molecules remain oriented to the field as they pass through these regions is dependent on the properties of the electric fields. Polar molecules typically follow the field adiabatically, and the adiabatic eigenstates can be quantized with respect to the axis of the electric field vector. The probability of a nonadiabatic transition occurring as molecules pass through different electric fields is dependent on a number of factors. Nonadiabatic transitions can occur when a molecule is not able to follow the changes in the electric field direction, such as when the frequency at which an electric field is rotated is comparable to the splitting between neighbouring  $M$  states, or when the molecule passes rapidly through a zero-field crossing, as described in Landau–Zener theory. Such situations are generally avoided inside the quadrupole guide, as the rate of rotation of the field is orders of magnitude slower than the minimum splitting between states ( $1.9 \times 10^9 \text{ rad s}^{-1}$  in  $\text{ND}_3$ , at a field of  $2 \text{ kV cm}^{-1}$ ) [13]. However, in situations where the magnitude of the electric field is minimal, there is a near-degeneracy in states differing only in their orientation with respect to the electric field. At zero field, the ammonia energy levels are no longer split by the Stark effect – although the manifold is not entirely degenerate, owing to the presence of inversion and hyperfine splittings.

To maintain their orientation to the local field, molecules must follow the field adiabatically. It has been demonstrated that nonadiabatic transitions can be largely suppressed in an ensemble of trapped ammonia molecules through the use of an electrostatic trap with a non-zero field minimum at the trap centre [14]. This study also notes that nonadiabatic transitions are minimised when only the magnitude of the field – and not the direction – changes

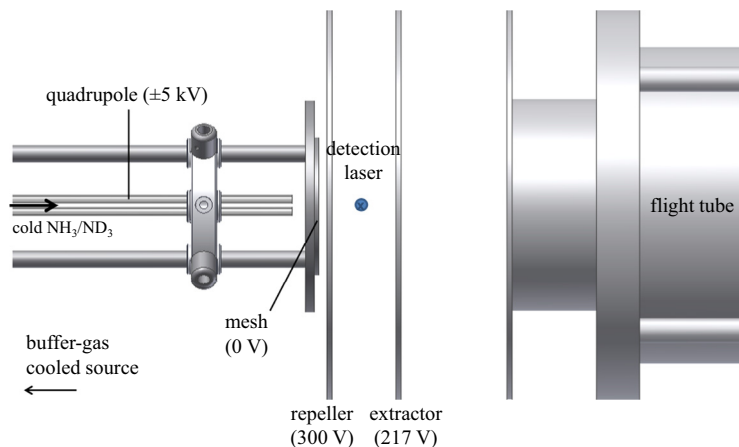


Fig. 1. Schematic illustration of the detection region in the experimental apparatus.

rapidly [14]. Hence the longer the molecules spend in near-zero field regions, and the higher the rate at which the field direction changes, the greater the probability of a nonadiabatic transition occurring and thus a loss of orientation to the local field.

To probe the orientation of ammonia molecules,  $(2 + 1)$  REMPI spectra are recorded using linearly polarised light. The polarisation of the REMPI laser can be controlled such that it is parallel or perpendicular to the ToF axis, using a  $\lambda/2$  waveplate and a polarising beam splitter. The use of linearly polarised light facilitates the probing of the  $M$  distribution, and thus the orientation of molecules at the point of spectroscopic probing. For a two-photon transition,  $\Delta M = 0, \pm 2$  transitions are excited by photons polarised perpendicular to the field gradient; only  $\Delta M = 0$  transitions are excited by parallel light.

### 3. Results and discussion

#### 3.1. Quantum state populations

$(2 + 1)$  REMPI spectra are recorded by exciting the  $\tilde{B}(\nu'_2 = 5) \leftarrow \tilde{X}(\nu'_2 = 0)$  transition in  $\text{ND}_3$  and  $\text{NH}_3$ . As can be seen in Fig. 2, there are clear differences in the intensities of many of the transitions when comparing spectra recorded with parallel and perpendicular linearly polarised light. These consistent and significant differences in intensity arise due to the preferential orientation of ammonia molecules to the local field at the point of spectroscopic probing. The laser polarisation axis is the only parameter that is changed between the two spectra, and no other known factor is believed to affect the intensities in this manner. If the  $M$ -state distribution was entirely isotropic then there would be no differences in peak intensities between the parallel and perpendicular polarisations. Numerous repeat scans have been recorded over a shorter spectral range; the 63,008–63,028  $\text{cm}^{-1}$  (two-photon energy) region of the  $\text{ND}_3$  REMPI spectrum is chosen for examination as it exhibits several isolated transitions and the peak intensities display a strong dependence on the laser polarisation direction.  $\text{ND}_3$  also has a greater transmission efficiency through the electrostatic guide, yielding spectra with an enhanced signal-to-noise ratio when compared to  $\text{NH}_3$  [15], hence the analysis focuses on  $\text{ND}_3$ .

The PGOPHER spectral fitting and simulation software package [16] is employed to simulate spectra under different polarisation conditions and thus determine the distribution over  $J$ ,  $K$  and  $M$ . The simulations are performed assuming a very small static electric field ( $1 \text{ V m}^{-1}$ ), which has a negligible effect on its own on line positions or overall intensities, but forces each  $M$  component to be

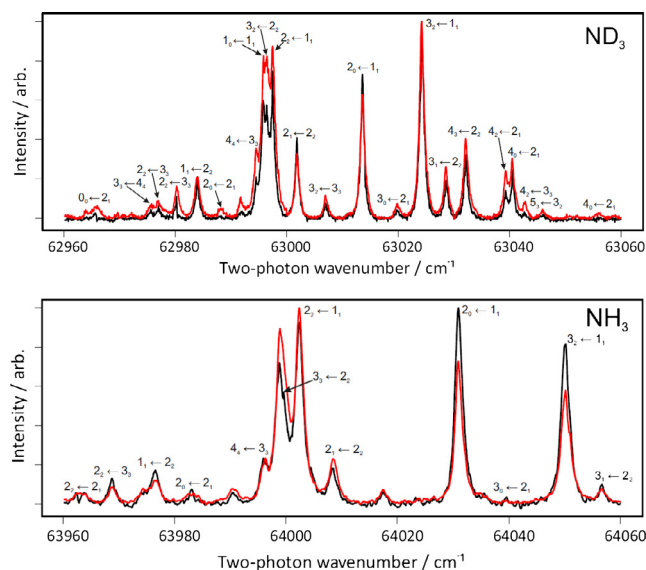


Fig. 2. Experimental  $(2 + 1)$  REMPI spectra of  $\text{ND}_3$  and  $\text{NH}_3$ , recorded with the laser polarisation axis aligned parallel (black) and perpendicular (red) to the electric field axis. Each of the four spectra are normalised to the total integrated intensity in the spectral region, and transitions are labelled as  $J_K$ . (For interpretation of the references to colour in this figure legend, the reader is referred to the web version of this article.)

calculated separately. A small addition to the PGOPHER program was required to extract the desired information from the spectra shown here, and the need for this can be seen by considering the spherical tensor form of the interaction of a molecule with an electric field,

$$-\sum_k \mathbf{T}^k(\mu) \cdot \mathbf{T}^k(E) = -\sum_k \sum_p (-1)^p T_p^k(\mu) T_{-p}^k(E). \quad (1)$$

Here,  $k$  is the rank of the interaction and  $p$  the component; for this work we only require  $k = 2$ , and ignore any quantum number dependence of the ionisation step.  $T_p^k(E)$  describes the laser field and  $T_p^k(\mu)$  is the transition moment operator, whose matrix elements give rise to the quantum number dependence of the transition intensity – which includes a dependence on  $M$ . This  $M$  dependence is independent of molecule type, and is simply given by a  $3-j$  symbol involving  $M$  and the total angular momentum,  $J$ .

While typically unimportant (providing the distribution of population over  $M$  states is uniform), the  $M$  dependence must be

specifically included here. The selection rule on  $M$  is determined by  $p$  (as  $M' - M = p$ ), and for rank 2 transitions three values of  $p$  must be included:  $-2$ ,  $0$  and  $+2$ . The relative weightings must also be considered, and these can be found by considering the Cartesian forms of the second rank electric field tensor formed by coupling the first rank electric field vector with itself if only one component of the field is non-zero. If only  $E_z \neq 0$  (described as a parallel transition), then

$$T_0^2(E) = \frac{2E_z^2}{\sqrt{6}}. \quad (2)$$

If only  $E_x \neq 0$  (described as a perpendicular transition), then

$$T_0^2(E) = \frac{-E_x^2}{\sqrt{6}}; \quad T_{\pm 2}^2(E) = \frac{E_x^2}{2}. \quad (3)$$

(Note that  $E_y$  has a different sign for  $p = \pm 2$ , but is otherwise identical to  $E_x$ .) An important difference here is that two different values of  $|p|$  must be included for perpendicular polarisation, in contrast to the one photon case where only one is required. This more general case, including the relative weightings shown above, has been added to version 10 of the **PGOPHER** program for the calculation of the polarisation dependent,  $M$ -dependent REMPI intensities – in fact, in a more general form using the formula for coupling tensor operators to allow for arbitrary rank.

The simulations are completed by specifying the population of each level as a separate (fitted) parameter, rather than using the Boltzmann default. A contour fit is performed for spectra recorded over the 63,008–63,028  $\text{cm}^{-1}$  region, with the spectroscopic constants fixed to literature values [17,18] and the rotational populations floated. The only variable in fitting the experimental spectra is the population of each  $J$ ,  $K$  and  $M$  state. The populations that are returned from this fitting procedure are robust – as illustrated by the excellent agreement between the experimental and simulated spectra (see Fig. 3).

The  $MK$ -state populations obtained from the experimental spectra are provided in Table 1, normalised within each  $J_K$  state, and the relative populations of the different states  $MK$  within a given  $J_K$  state. Note that states with the same product  $MK$  (i.e.  $-1 + 1$  and  $+1 - 1$ ) are degenerate and so are not distinguished in our analysis. The data provide a straightforward comparison with the statistical  $MK$ -state populations (i.e. the population expected if there is no orientation of molecules to the external field axis). It should be emphasised that the “perpendicular” and “parallel” spectra provide independent measurements – in excellent agreement – of the

**Table 1**

Relative  $\text{ND}_3$  rotational state populations established from **PGOPHER** fits to the experimental spectra recorded with different laser polarisations. Populations are normalised such that the population within each  $J_K$  state sums to 1. Statistical populations are provided for comparison.

$ J,  K , MK\rangle$	Perpendicular	Parallel	Statistical
$ 1, 1, -1\rangle$	0.22(15)	0.20(16)	0.33
$ 1, 1, 0\rangle$	0.38(8)	0.39(8)	0.33
$ 1, 1, 1\rangle$	0.40(13)	0.40(14)	0.33
$ 2, 1, -2\rangle$	0.28(11)	0.34(16)	0.20
$ 2, 1, -1\rangle$	0.21(8)	0.18(3)	0.20
$ 2, 1, 0\rangle$	0.12(11)	0.11(11)	0.20
$ 2, 1, 1\rangle$	0.13(10)	0.11(10)	0.20
$ 2, 1, 2\rangle$	0.26(8)	0.26(8)	0.20
$ 2, 2, -4\rangle$	0.26(3)	0.25(5)	0.20
$ 2, 2, -2\rangle$	0.21(8)	0.18(6)	0.20
$ 2, 2, 0\rangle$	0.17(8)	0.18(8)	0.20
$ 2, 2, 2\rangle$	0.14(7)	0.14(7)	0.20
$ 2, 2, 4\rangle$	0.22(4)	0.26(8)	0.20

$|J, K, M\rangle$  population distribution. Very conservative uncertainties are reported for the experimental populations, arising from the weak  $M$ -state dependence of the transitions. The error bounds are determined by varying the populations until an integrated peak area  $\pm 5\%$  of a given experimental peak area is achieved, to ensure that the extent of variation in the experimental intensities over numerous runs is completely accounted for. The agreement of the independently measured “perpendicular” and “parallel” population distribution is well within the stated uncertainty in all instances. However, a clear difference is evident and consistently reproducible when comparing the experimental  $MK$ -state populations with the statistical distribution, providing further evidence that the residual orientation observed in the spectra is a real effect.

To interpret how the molecules maintain some residual orientation, and to establish whether a more complete orientation could be achieved, trajectory simulations are performed. The  $MK$ -state distribution at the exit of the quadrupole is established, and the orientational probability distribution is calculated as the molecules pass through the post-quadrupole field regions, by propagation of the time-dependent Schrödinger equation (TDSE).

### 3.2. Simulations

The electric fields that the ammonia molecules experience as they pass through the quadrupole guide and into the ionisation region are modelled using **SIMION** [19], and are depicted in Fig. 4. Voltages are applied to each element of the experimental apparatus (see Fig. 1) and the Laplace equation is solved, enabling the electric fields to be calculated. Three potential arrays are used to model the experimental components of interest: the final section of the quadrupole guide, the grounded mesh, and the time of flight tube. The Ni mesh (wire width 12.7  $\mu\text{m}$ , pore area 0.042  $\text{mm}^2$ , 88% transmittance) is described fully to account for any micro-focusing and fringe fields. Voltages are applied to the quadrupole guide and the repeller and extractor plates throughout the simulations, in accordance with the experimental conditions.

A **MATLAB** [20] program propagates  $\text{ND}_3$  molecules with a pre-defined initial quantum state and velocity through the fields of the experimental apparatus. The quantum state of each  $\text{ND}_3$  molecule, determined from the TDSE propagation, is monitored as a function of time, facilitating an analysis of the effect that different field regions have on the orientation of the molecules. The electric fields within the quadrupole are inhomogeneous, with the local field vectors perpendicular to the ToF axis (the  $z$ -axis); the quantization axis of the static field in the detection region is parallel to the  $z$ -axis.

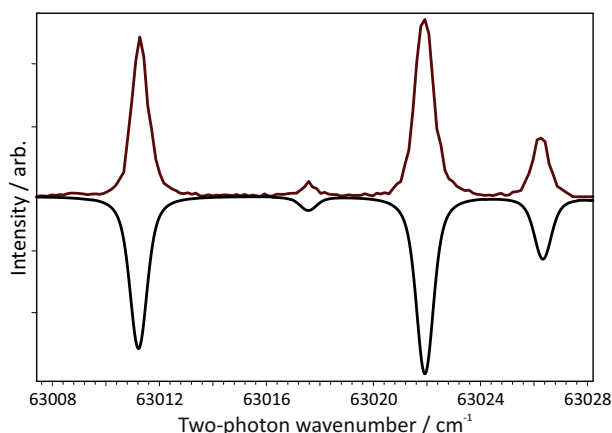


**Fig. 3.** Experimental (above) and simulated (inverted, below)  $\text{ND}_3$  (2 + 1) REMPI spectrum, recorded over the region 63008–63028  $\text{cm}^{-1}$  (two-photon energy) with the laser polarisation axis parallel to the local electric field.



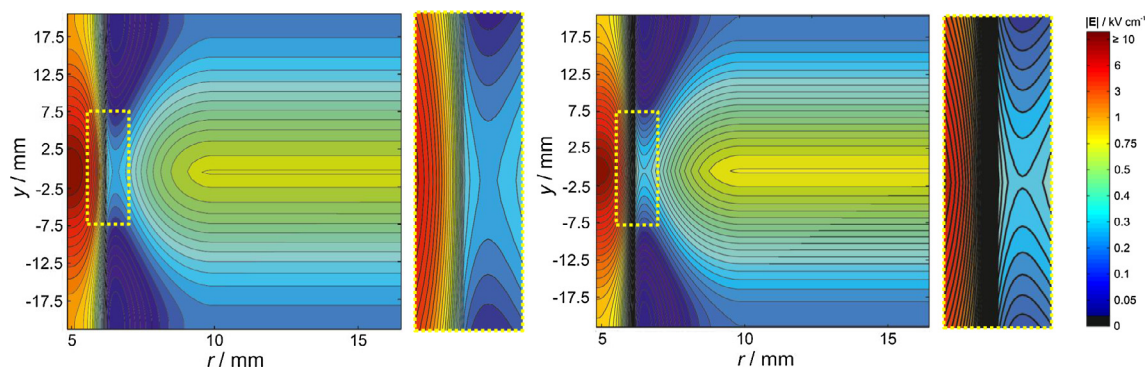


**Fig. 4.** 2D slices showing the electric fields in the apparatus, with a bias of 17 V applied to the mesh (left) and with the mesh held at 0 V (right). The regions enclosed within the dashed yellow lines are provided enlarged beside each plot, to better show the influence of applying a small positive voltage to the mesh (left) and holding the mesh at ground (right). The quadrupole guide exit is at 0 mm, with the mesh located at 6.05 mm and the repeller plate at 8.00 mm. (For interpretation of the references to colour in this figure legend, the reader is referred to the web version of this article.)

An ensemble of  $10^5$   $\text{ND}_3$  molecules in the rotational states  $J_K = 1_1, 2_1$  and  $2_2$  (corresponding to the states observed experimentally in the spectral region of interest) and with a velocity of  $70.29 \text{ m s}^{-1}$  (corresponding to the modal velocity determined experimentally [11]) is propagated through the different electric field regions. The symmetric top basis set is employed, with the inclusion of inversion doubling and hyperfine interactions. The hyperfine parameters within the Hamiltonian are taken from van Veldhoven et al. [21], enabling the splitting and shifting of the various energy levels in the manifold (in the presence of an external electric field) to be calculated using a tensor coupling scheme [21,22]. The time-dependent Schrödinger equation is solved in a co-ordinate system that rotates with the field direction, as this is more efficient than considering a rotating field in a fixed co-ordinate system, as demonstrated by Wall et al. [13]. This is achieved through the use of a rotation operator, with the time evolution of the Schrödinger equation in the rotating frame subsequently expressed in a basis set of the instantaneous eigenvectors. As set out by Wall et al. [13], such an approach enables the effect of the rotation of the electric field and changes in the field magnitude to be evaluated. As the rate of rotation of the field experienced by a molecule as it moves through the apparatus is generally very low compared to the rotational frequency of the molecule or the Stark frequency differences of the  $M$  states, the field rotation does not induce population changes except when the field is very low, *i.e.* the states follow the field direction adiabatically. However, as discussed below, the region near the entry to the mesh is an exception in that the field rotates relatively rapidly in a near-zero field situation.

The time evolution of the Stark Hamiltonian is tracked at time steps of 20 ns, enabling the  $M$ -state population evolution to be recorded. This yields the orientation of the molecules to the local electric field. (Note that the quantum number  $M$  is the projection of  $J$ , while the time evolution is calculated for a basis set defined in terms of an  $M_F$  quantum number [see below]; a back-transformation is therefore required to determine the  $M$ -state populations.) Within the quadrupole guide,  $\text{ND}_3$  molecules are oriented by an inhomogeneous local electric field. The orientation of molecules with respect to a fixed laboratory axis can be established by transforming the angular momentum from a local field frame to a space-fixed frame [23], as set out in the orientational probability distribution functions introduced by Choi and Bernstein [24]. When a rotation acts on the eigenstate  $|JM\rangle$  of  $\mathbf{J}^2$  and  $J_z$ , it transforms  $|JM\rangle$  into a linear combination of other  $M$  values using a rotation matrix. A rotation transforms the system from the original  $(X, Y, Z)$  frame to a new  $(X', Y', Z')$  frame, with a common origin. This allows the probability of  $\mathbf{J}$  making the projection  $M'$  onto

new axis  $Z'$  (corresponding to the fixed laboratory  $z$  axis) to be calculated using rotation matrices, as described by Zare [23].

The orientation of  $\text{ND}_3$  molecules ( $MK$ -state description) is plotted as a function of position in Fig. 5, showing how the molecular orientation changes as particles pass through the various regions. The  $MK$ -state distributions are presented in the local field frame (*i.e.* where the molecules are oriented to the local electric field), alongside the orientation of molecules with respect to the fixed laboratory  $z$  axis, parallel to the quadrupole axis. The simulations show that the  $M$ -state distribution within the quadrupole guide is retained as the molecules exit the guide (0–6 mm), but is rapidly lost as the molecules pass through the grounded mesh (located 6.05 mm beyond the guide exit). This is because of nonadiabatic transitions, due primarily to the very rapid field rotation that occurs (radial to axial) as the molecule enters the near-zero field region and subsequently due to the significant length (and hence time) over which the molecules are held near zero field.

While the mesh itself is very thin, with the Ni wire only 0.1 mm thick, the mesh holder has a width of 1.0 mm. Both the mesh and the mesh holder are held at ground during the experiments. As a result, molecules experience regions of near-zero electric field for a  $z$ -axis distance of up to 1.1 mm. The potentials around the region of the mesh are depicted in Fig. 6, where the magnitude of the electric field can be seen to fall to  $\leq 50 \text{ mV cm}^{-1}$  within  $200 \mu\text{m}$  of entering the mesh.

After passing through the mesh, molecules in the  $1_1$  state experience complete loss of orientation; *i.e.* a statistical population distribution is seen at a distance of 7.15 mm after the guide exit. It is interesting to observe that the transfer of population from the  $|1, -1\rangle$  state to either the  $|1, 0\rangle$  state or the  $|1, 1\rangle$  state occurs at the same rate. One might expect, due to the inversion splitting and thus lack of total degeneracy at zero field, that population would be transferred to the  $|1, 0\rangle$  state in preference to the  $|1, 1\rangle$  state. This is, in fact, the behaviour observed if an artificially large inversion splitting is implemented. Employing the inversion splitting reported for  $\text{NH}_3$ ,  $0.792 \text{ cm}^{-1}$  [25], sees the majority of molecules oriented to the local field: the population in  $|1, -1\rangle$  is  $\sim 74\%$  at the point of ionisation, with 23% in the  $|1, 0\rangle$  state and 3% in  $|1, 1\rangle$ . (The Stark shifts for the  $J = 1$  and  $J = 2$  states in  $\text{NH}_3$  and  $\text{ND}_3$  are provided in Fig. 7.) Thus the small magnitude of the inversion splitting in  $\text{ND}_3$  (at only  $0.053 \text{ cm}^{-1}$  [25]), in addition to the very rapid field rotation, also plays a role in determining the extent of de-orientation as molecules pass through regions of near-zero field.

Some molecules in  $J = 2$  maintain their orientation in the local field frame, with the population in  $|J, MK\rangle = |2, -2\rangle$  and  $|2, -4\rangle$  at 7.15 mm greater than that expected from a purely statistical distribution. While inspection of Fig. 7 reveals that the inversion

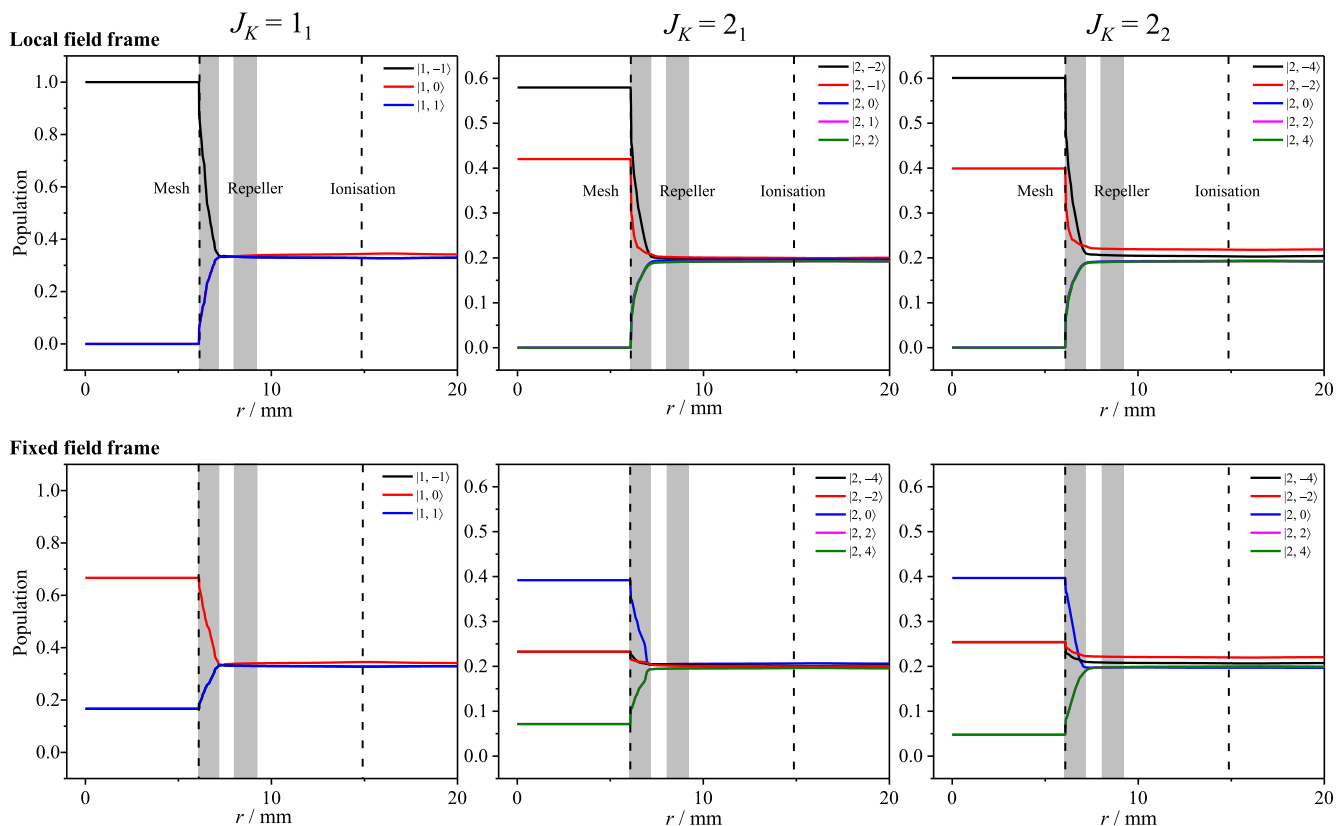


**Fig. 5.** The orientation of  $\text{ND}_3$  molecules as they pass through the experimental apparatus is monitored using trajectory simulations. The guide exit is located at 0 mm, with the grounded mesh located from 6.05 to 6.15 mm, with the mesh holder extending a further 1.0 mm. The repeller plate extends from 8.00 to 9.20 mm. Molecules are probed by the REMPI laser 14.85 mm beyond the guide exit. The top row represents the  $|J, MK\rangle$  populations in the local field frame, providing the orientation of molecules with respect to the local electric field. The bottom row illustrates the orientation of molecules with respect to a fixed laboratory axis, parallel to the quadrupole axis. As  $M$  is defined with respect to the local electric field, and not a space-fixed axis, the lower panel plots the  $M'$  distribution. (At distances beyond the repeller,  $M' \equiv M$  as the electric field vector aligns with the  $z$  axis.)

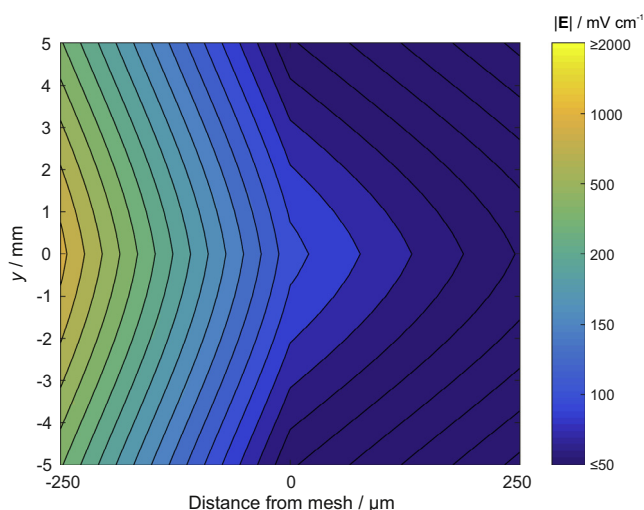


**Fig. 6.** 2D slice illustrating the near-zero electric fields in the region around the mesh, with all voltages applied as in the experiments (i.e. with the mesh grounded). The distance axis is depicted with respect to the position of the mesh, with the  $y$  axis directly comparable to that in Fig. 4. Note that the colour scale has been altered from that adopted for Fig. 4, as the fields here are on the order of tens to hundreds of  $\text{mV cm}^{-1}$ .

splitting in the  $2_2$  state of  $\text{ND}_3$  is the same as for the  $1_1$  state, the magnitude of the Stark splitting in the  $|2, -4\rangle$  level is greater than that observed for the  $|1, -1\rangle$  level, at a given electric field.

However, the picture is not quite as straightforward as this; the  $J = 2$  Stark map has the added complexity of additional  $MK$  states. Within the  $J_K = 2_2$  manifold, population appears to initially decay fastest from the  $|J, MK\rangle = |2, -2\rangle$  state, but after a short distance the loss rate from this state reduces significantly. The change in population of a given low-field seeking state is unlikely to be described by a single exponential decay rate (given the complicated hyperfine structure of  $\text{ND}_3$ ). Nonetheless, the population change in the  $|2, -2\rangle$  state is more complicated than for the  $|1, -1\rangle$  or  $|2, -4\rangle$  levels – owing to the added possibility of population transferring into the  $|2, -2\rangle$  state from the adjacent  $|2, -4\rangle$  state.

At a distance of 8.00 mm beyond the quadrupole guide exit, molecules pass through a repeller plate and into a region of uniform electric field. The repeller plate is held at a constant voltage of 300 V, with the extractor plate (located at 23.00 mm) held at 217 V. There are minor changes to the orientation of molecules in the uniform field of the ionisation region – in the case of  $J_K = 1_1$  resulting in a slight enhancement in the  $MK = 0$  population over the  $MK = \pm 1$  states. This is in agreement with the populations obtained from the fits to the spectra, where a higher population is seen in the  $|J, |K|, MK\rangle = |1, 1, 0\rangle$  state compared to the  $|1, 1, -1\rangle$  level.

At the point of spectroscopic probing, our calculations confirm the experimental observation: that ammonia molecules exhibit some orientation to the local field. Molecules in the  $2_2$  state retain some orientation from the quadrupole guide, and molecules in the  $1_1$  state exhibit minor orientation to the static repeller and extractor fields. As the magnitude of fringe fields emanating from the

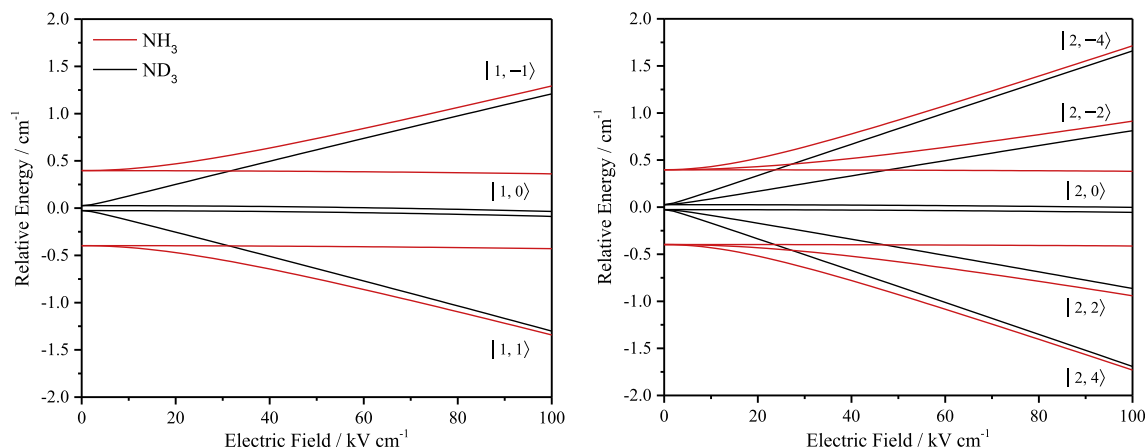


**Fig. 7.** The Stark splitting in the  $j = 1$  and  $j = 2$  states of  $\text{NH}_3$  (red) and  $\text{ND}_3$  (black), plotted as a function of electric field, with states labelled as  $|j, MK\rangle$ . (For interpretation of the references to colour in this figure legend, the reader is referred to the web version of this article.)

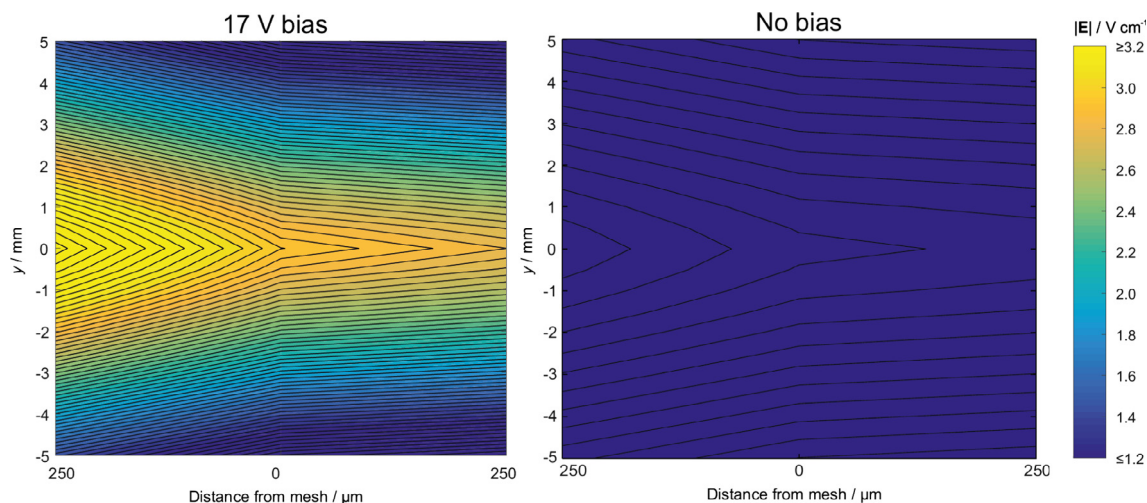


**Fig. 8.** 2D slices showing the electric fields in the region around the mesh, again with a bias of 17 V applied to the mesh (left) and with the mesh held at 0 V (right). While the mesh itself is not depicted, the effect of the mesh can be seen in the change in the field lines at 0  $\mu\text{m}$ . Note that the colour scale has again been altered from those adopted for Figs. 4 and 6, to highlight the difference that a 17 V bias applied to the mesh makes to the fields in this region. (For interpretation of the references to colour in this figure legend, the reader is referred to the web version of this article.)

quadrupole guide – and the extent to which they can penetrate beyond the mesh – is small, they are insufficient to maintain the orientation of the majority of ammonia molecules for any appreciable distance beyond the mesh. The calculations appear to under-estimate the degree of orientation that is seen experimentally. This could arise if, for example, the voltage on the mesh is not exactly zero in the experiments, as any small positive voltage applied to the mesh has a significant effect on the orientation of ammonia molecules.

### 3.3. Maintaining orientation through the detection region

The orientation of molecules as they exit a hexapole guide and enter a region of uniform field has been previously studied, with fields as low as  $3 \text{ V cm}^{-1}$  sufficient to orient  $\text{CH}_3\text{I}$  molecules to the external field axis [12,26]. While the behaviour of  $\text{ND}_3$  under such conditions has not been reported,  $\text{ND}_3$  exhibits many similar properties to  $\text{CH}_3\text{I}$ : both molecules are symmetric tops with  $C_{3v}$  symmetry and have comparable permanent dipole moments (1.6 D for  $\text{ND}_3$  and 1.5 D for  $\text{CH}_3\text{I}$ ) [27,28], although  $\text{ND}_3$  exhibits a far

more complex manifold of hyperfine states with the added complication of inversion splitting.

In the simulations undertaken in this work, varying voltages can be applied to the mesh to establish the minimum field needed to orient ammonia molecules at the point of ionisation. With the application of a small bias voltage to the mesh, resulting in a field of just  $1 \text{ V cm}^{-1}$  at the position of the mesh (measured using SIMION, with the voltages applied to all other elements as in the experiments), 84% of  $\text{ND}_3$  molecules in  $J_K = 1_1$  adiabatically follow the field and retain their orientation through to the point of ionisation. The electric potentials are plotted in Fig. 4, illustrating the fields both with the mesh held at ground and with a bias voltage of 17 V applied to it (corresponding to a field of  $3 \text{ V cm}^{-1}$  at the mesh). The region around the mesh is shown in greater detail in Fig. 8. When the almost zero-field region at the mesh is removed, the near-homogeneous fields beyond the mesh rotate the local field experienced by the molecules, from the inhomogeneous field in the quadrupole to the uniform direction of the ionisation region field. This can be seen in Fig. 9, where the orientation of  $\text{ND}_3$  molecules in the molecular frame is preserved as they move through the different electric field regions.

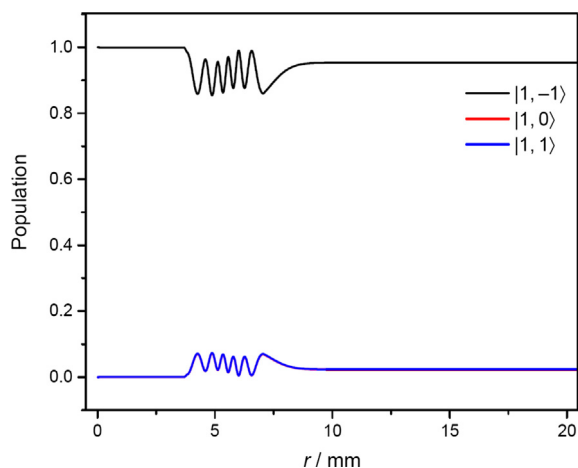


**Fig. 9.** Simulated fraction of total  $J_K = 1_1$  population in the  $|J, MK\rangle = |1, -1\rangle, |1, 0\rangle$  and  $|1, 1\rangle$  states (in the local field frame) as the molecules pass through the different field regions, with a bias voltage of 17 V applied to the mesh. It can be seen that the molecules follow the electric fields throughout the apparatus, resulting in almost complete orientation of molecules – over 95% of population in the  $|1, -1\rangle$  state – in the uniform field of the ionisation region. As such, orientation of  $> 95\%$  of  $\text{ND}_3$  molecules in the laboratory frame is achieved at the point of ionisation.

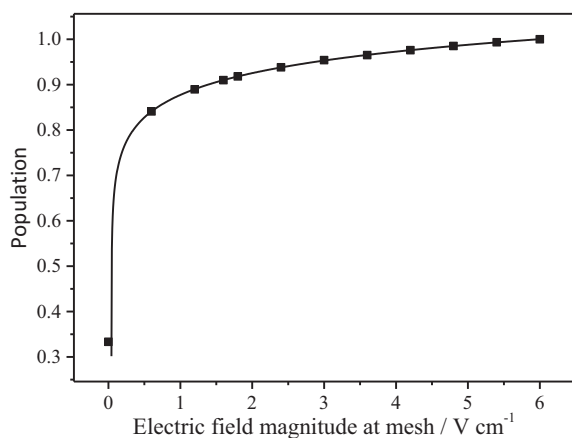


**Fig. 10.** Simulated fraction of total  $J_K = 1_1$  population in the  $|1, -1\rangle$  state at the point of ionisation, monitored as a function of the magnitude of the electric field at the mesh.

These simulations are in agreement with the significant orientation effects observed by Bernstein et al. with  $\text{CH}_3\text{I}$  molecules in fields as low as  $0.3 \text{ V cm}^{-1}$  [29,30]. As shown in Fig. 10, fields on the order of a few  $\text{V cm}^{-1}$  are sufficient to maintain  $> 90\%$  of population in the  $|1, -1\rangle$  state. The simulations suggest that over 95% of population will be retained in the  $|1, -1\rangle$  state when a 17 V bias voltage is applied to the mesh – in accordance with the observations of Harland et al. in their  $\text{CH}_3\text{I}$  study [26]. While the field rotation occurs just as rapidly with the removal of the near-zero field region, at a higher field the splitting between states is larger, hence nonadiabatic transitions are suppressed.

An alternative approach could see the mesh holder – currently made of stainless steel – replaced with an insulating material. The mesh itself has a width of only 0.1 mm; replacing the 1.00 mm-width mesh holder with an insulating material will significantly reduce the length of the near-zero field region along the  $z$  axis. As a result, molecules will spend less time in near-zero fields, reducing the probability of nonadiabatic transitions in this region and thus curtailing the loss of orientation to the local field – although losses due to the rapid rotation of the field between the

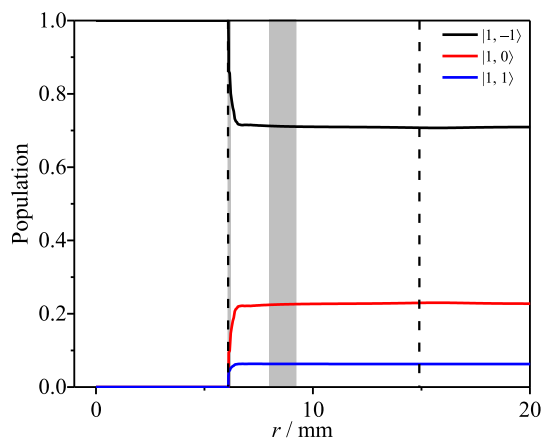


**Fig. 11.** Simulated fraction of total  $J_K = 1_1$  population in the  $|J, MK\rangle = |1, -1\rangle, |1, 0\rangle$  and  $|1, 1\rangle$  states (in the local field frame) as the molecules pass through the apparatus, with the previously stainless steel mesh holder replaced by an insulating material. Only the 0.1 mm-thick mesh is held at 0 V, resulting in a reduced near-zero field region and retention of over 70% of population in the  $|1, -1\rangle$  state.

quadrupole and the mesh will still occur. Simulations indicate that replacing the mesh holder with an insulating material will result in the orientation of 70% of ammonia molecules at the detection region, as depicted in Fig. 11.

#### 4. Conclusion

Ammonia molecules exiting an electrostatic quadrupole guide and passing through a grounded mesh into a reaction chamber exhibit some orientation to the local electric field. It is, however, easy to lose orientation when molecules pass through near-zero field regions; fields need to be designed to preserve the orientation of molecules throughout the apparatus. Simulations indicate that the application of a small bias voltage to the (typically grounded) mesh could result in full orientation of  $\text{ND}_3$  molecules at the point of interrogation. A linear Paul ion trap has been installed in place of the repeller and extractor plates to facilitate the study of cold, controlled ion-molecule reactions. In the combined quadrupole guide-ion trap experiments, the mesh will serve an important role in shielding the ion trap from the significant voltages applied to the quadrupole electrodes. Simulations are underway to establish the effect that applying a small bias voltage to the mesh will have on the trapping fields applied to the ion trap electrodes. An alternative approach could see the replacement of the stainless steel mesh holder with an insulating material, which will curtail the loss of orientation by reducing the length of the near-zero field region.

To preserve the orientation of molecules as they enter the ion trap, one would need to prevent the radiofrequency trapping fields from inducing nonadiabatic transitions. This could be achieved through the use of digital trapping waveforms (also termed square-wave or pulsed waveforms), whereby a rectangular waveform of period  $T$  and pulse width  $\tau$  is employed. The digital waveform is zero when  $\tau T/2 < |t| \leq (1 - \tau)T/2$  and  $(1 + \tau)T/2 < |t| \leq (2 - \tau)T/2$ . This “off time” can be extended by switching off the trapping fields for a short time, allowing the oriented molecules to be admitted to the trapping region without adverse fields being present, although there are still challenges associated with molecules entering the trap at zero field. If a compromise can be achieved between shielding the ion trap from external fields and maintaining the orientation of the ammonia molecules as they pass through the region, this will enable the examination of ion-molecule reactions with unprecedented control over the reaction parameters.



## Acknowledgements

TPS acknowledges the financial support of the EPSRC (projects EP/E00224X/1 and EP/I029109/1) and the Wiener Anspach Foundation. BRH is grateful for support from the Leverhulme Trust. TPS, BRH and LSP acknowledge support from the Marie Curie Initial Training Network scheme (COMIQ, FP7-GA-607491). Supporting data can be obtained from the Oxford Research Archive.

## References

- [1] D. Skouteris, D.E. Manolopoulos, W.S. Bian, H.-J. Werner, L.-H. Lai, K.P. Liu, *Science* 286 (1999) 1713.
- [2] N. Balakrishnan, *J. Chem. Phys.* 121 (2004) 5563.
- [3] D.H. Parker, R.B. Bernstein, *Annu. Rev. Phys. Chem.* 40 (1989) 561.
- [4] T.P. Rakitzis, A.J. van den Brom, M.H.M. Janssen, *Science* 303 (2004) 1852.
- [5] V. Aquilanti, M. Bartolomei, F. Pirani, D. Cappelletti, F. Vecchiocattivi, Y. Shimizu, T. Kasai, *Phys. Chem. Chem. Phys.* 7 (2005) 291.
- [6] P.R. Brooks, *Science* 193 (1976) 11.
- [7] M.H.G. de Miranda, A. Chotia, B. Neyenhuis, D. Wang, G. Quemener, S. Ospelkaus, J.L. Bohn, J. Ye, D.S. Jin, *Nat. Phys.* 7 (2011) 502.
- [8] J. Jankunas, K.S. Reisman, T.P. Rakitzis, A. Osterwalder, *Mol. Phys.* 114 (2016) 245.
- [9] K. Schreel, J.J. ter Meulen, *J. Phys. Chem. A* 101 (1997) 7639.
- [10] C. Sommer, L.D. van Buuren, M. Motsch, S. Pohle, J. Bayerl, P.W.H. Pinkse, G. Rempe, *Faraday Discuss.* 142 (2009) 203.
- [11] K.S. Twyman, M.T. Bell, B.R. Heazlewood, T.P. Softley, *J. Chem. Phys.* 141 (2014) 024308.
- [12] P.R. Brooks, E.M. Jones, K. Smith, *J. Chem. Phys.* 51 (1969) 3073.
- [13] T.E. Wall, S.K. Tokunaga, E.A. Hinds, M.R. Tarbutt, *Phys. Rev. A* 81 (2010) 033414.
- [14] M. Kirste, B.G. Sartakov, M. Schnell, G. Meijer, *Phys. Rev. A* 79 (2009) 051401 (R).
- [15] E.W. Steer, K.S. Twyman, B.R. Heazlewood, T.P. Softley, *Mol. Phys.* 113 (2015) 1465.
- [16] C.M. Western, PGOPHER: a program for simulating rotational, vibrational and electronic spectra, *J. Quant. Spectrosc. Radiat. Transfer* 186 (2016) 221–242.
- [17] S. Urban, D. Papousek, M. Bester, K. Yamada, G. Winnewisser, *J. Mol. Spectrosc.* 106 (1984) 29.
- [18] J. Bentley, B.J. Cotterell, A. Langham, R.J. Strickland, *Chem. Phys. Lett.* 332 (2000) 85.
- [19] D. Manura, D. Dahl, SIMION 8.0 User Manual, Scientific Instrument Services, Inc., Ringoes, NJ, 2008. 08551 <<http://simion.com/>>.
- [20] MATLAB R2013a, The MathWorks, Inc., Natick, Massachusetts, United States.
- [21] J. van Veldhoven, R.T. Jongma, B. Sartakov, W.A. Bongers, G. Meijer, *Phys. Rev. A* 66 (2002) 032501.
- [22] J. van Veldhoven, J. Kupper, H.L. Bethlem, B. Sartakov, A.J.A. van Roij, G. Meijer, *Eur. Phys. J. D* 31 (2004) 337.
- [23] R.N. Zare, *Angular Momentum*, Wiley, New York, 1988.
- [24] S.E. Choi, R.B. Bernstein, *J. Chem. Phys.* 85 (1986) 150.
- [25] C.H. Townes, A.L. Schawlow, *Microwave Spectroscopy*, Dover Publications, New York, 1975.
- [26] P.W. Harland, W.P. Hu, C. Vallance, P.R. Brooks, *Phys. Rev. A* 60 (1999) 3138.
- [27] C. Reichardt, T. Welton, *Solvents and Solvent Effects in Organic Chemistry*, Wiley-VCH, Weinheim, Germany, 2011.
- [28] K. Tanaka, H. Ito, T. Tanaka, *J. Chem. Phys.* 87 (1987) 1557.
- [29] R.B. Bernstein, S.E. Choi, S. Stolte, *J. Chem. Soc. Faraday Trans. 2* 85 (1989) 1097.
- [30] S.R. Gandhi, R.B. Bernstein, *J. Chem. Phys.* 93 (1990) 4024.